HHS Public Access

Author manuscript

J Mol Cell Cardiol. Author manuscript; available in PMC 2016 October 01.

Published in final edited form as:

J Mol Cell Cardiol. 2015 October ; 87: 248–256. doi:10.1016/j.yjmcc.2015.08.006.

Phosphorylation Sites in the Hook Domain of $Ca_V\beta$ Subunits Differentially Modulate $Ca_V1.2$ Channel Function

Sylvain Brunet[1,2,*], **Michelle A. Emrick**[1,*], **Martin Sadilek**[3], **Todd Scheuer**[1], and **William A. Catterall**[1]

[1]Department of Pharmacology, University of Washington, Seattle, WA 98195

[2]Department of Neurosciences, Cleveland Clinic Organization, Cleveland, OH 44195

[3]Department of Chemistry, University of Washington, Seattle, WA 98195

Abstract

Regulation of L-type calcium current is critical for the development, function, and regulation of many cell types. $Ca_V1.2$ channels that conduct L-type calcium currents are regulated by many protein kinases, but the sites of action of these kinases remain unknown in most cases. We combined mass spectrometry (LC-MS/MS) and whole-cell patch clamp techniques in order to identify sites of phosphorylation of $Ca_V\beta$ subunits in vivo and test the impact of mutations of those sites on $Ca_V1.2$ channel function in vitro. Using the $Ca_V1.1$ channel purified from rabbit skeletal muscle as a substrate for phosphoproteomic analysis, we found that Ser^{193} and Thr^{205} in the HOOK domain of $Ca_V\beta_{1a}$ subunits were both phosphorylated in vivo. Ser^{193} is located in a potential consensus sequence for casein kinase II, but it was not phosphorylated in vitro by that kinase. In contrast, Thr^{205} is located in a consensus sequence for cAMP-dependent phosphorylation, and it was robustly phosphorylated in vitro by PKA. These two sites are conserved in multiple $Ca_V\beta$ subunit isoforms, including the principal $Ca_V\beta$ subunit of cardiac $Ca_V1.2$ channels, $Ca_V\beta_{2b}$. In order to assess potential modulatory effects of phosphorylation at these sites separately from effects of phosphorylation of the $\alpha_1 1.2$ subunit, we inserted phosphomimetic or phosphoinhibitory mutations in $Ca_V\beta_{2b}$ and analyzed their effects on $Ca_V1.2$ channel function in transfected nonmuscle cells. The phosphomimetic mutation $Ca_V\beta_{2b}{}^{S152E}$ decreased peak channel currents and shifted the voltage dependence of both activation and inactivation to more positive membrane potentials. The phosphoinhibitory mutation $Ca_V\beta_{2b}{}^{S152A}$ had opposite effects. There were no differences in peak $Ca_V1.2$ currents or voltage dependence between the phosphomimetic mutation $Ca_V\beta_{2b}{}^{T164D}$ and the phosphoinhibitory mutation $Ca_V\beta_{2b}{}^{T164A}$. However, calcium-dependent inactivation was significantly increased for the phosphomimetic mutation $Ca_V\beta_{2b}{}^{T164D}$. This effect was subunit-specific, as the corresponding

Corresponding Author: William A. Catterall, wcatt@uw.edu, Tel. 206-543-1925, Fax 206-543-0388.

*Co-First Authors

Present Address: M.A.E, CMC ICOS Biologics, 22021 20th Ave SE, Bothell, WA 98021

Disclosures

None

mutation in the palmitoylated isoform, $Ca_V\beta_{2a}$, had no effect. Overall, our data identify two sites of conserved phosphorylation of the HOOK domain of $Ca_V\beta$ subunits in vivo and reveal differential modulatory effects of phosphomimetic mutations in these sites. These results reveal a new dimension of regulation of $Ca_V1.2$ channels through phosphorylation of the HOOK domains of their β subunits.

Keywords

L-type Ca^{2+} channel; Ventricular Myocytes; Electrophysiology

1. Introduction

Protein kinases regulate L-type calcium currents conducted by voltage-gated (Ca_V) channels to precisely control numerous physiological functions of nerve and muscle cells. $Ca_V1.1$ and $Ca_V1.2$ channels are regulated by a number of protein kinases (PKA, CaMKII, AKT/PKB, PKC and PKG) [1, 2]. PKA phosphorylation is required for up-regulating L-type calcium currents through $Ca_V1.1$ and $Ca_V1.2$ channels in the fight-or-flight response [2-5], and CaMKII is essential for frequency-dependent potentiation [6]. Dysregulation of protein kinases is implicated in many pathological conditions [7-9]. Despite its importance in physiology and pathophysiology, the molecular mechanisms of regulation of $Ca_V1.1$ and $Ca_V1.2$ channels by protein phosphorylation remain incompletely understood.

$Ca_V1.1$ and $Ca_V1.2$ channels in nerve and muscle cells consist of a pore-forming α_1 subunit in association with $Ca_V\beta$, $Ca_V\alpha2\delta$, and possibly $Ca_V\gamma$ subunits [2, 10, 11]. Calmodulin (CaM), a ubiquitous Ca binding protein, is also associated with this protein complex [12]. $Ca_V\alpha_1$ subunits are composed of four homologous domains (I-IV) with six transmembrane segments (S1-S6) and a reentrant pore loop in each [2]. Multiple regulatory sites are located in the large C-terminal domain of $Ca_V1.1$ and $Ca_V1.2$ channels [13-16], which is subject to *in vivo* proteolytic processing near its center [13, 17-19]. An IQ motif in the proximal C-terminus is implicated in Ca/calmodulin-dependent inactivation [14, 15]. Noncovalent interaction of the distal C-terminus with the proximal C-terminal domain has an auto-inhibitory effect by reducing coupling efficiency of gating charge movement to channel opening [16, 20, 21], and the proximal C-terminus EF-hand is required to mediate the auto-inhibitory effect of the distal C-terminus [22]. Recently, it was shown that this autoinhibitory $Ca_V1.2$ signaling complex with an A Kinase Anchoring Protein bound is sufficient to recapitulate the stimulatory actions of PKA on $Ca_V1.2$ channels in a non-muscle cell system [23]. This reconstituted regulatory system has allowed functional tests of the role of phosphorylation sites in the α1 subunits in calcium channel regulation.

In our previous studies, we took advantage of the ease of purification of $Ca_V1.1$ channels from rabbit skeletal muscle to identify sites of in vivo phosphorylation of the α1 subunits [24]. We then used our reconstituted regulatory system to analyze the functional effects of mutations in the homologous sites in the $Ca_V1.2$ channel, which are highly conserved. We found that two conserved sites located at the interface between the distal and proximal C-terminal domains were required for regulation of basal and PKA-stimulated channel activity

[23]. Both a PKA site at Ser^{1700} and a casein kinase II site at Thr^{1704} were required for normal regulation of basal channel activity, whereas only Ser^{1700} was required for stimulation of channel activity by PKA [23]. These results suggest that PKA phosphorylation of $Ca_V1.2$ at Ser^{1700} relieves the autoinhibition of the distal C-terminal on $Ca_V1.2$ channel function allowing the PKA-dependent increase in current amplitude. Mice with mutations in Ser^{1700} and Thr^{1704} have greatly reduced basal L-type calcium currents and much reduced response to β-adrenergic stimulation [25, 26], as expected from these studies in transfected nonmuscle cells.

Phosphorylation sites in $Ca_V\beta$ subunits were identified previously by a variety of biochemical and proteomic techniques [18, 27-29], but the level of phosphorylation in vivo, and the physiological significance of these phosphorylation sites remain uncertain. In the experiments described here, we have used mass spectrometry (LC-MS/MS) of purified skeletal muscle $Ca_V1.1$ channels for phosphoproteomic analysis and whole-cell patch clamp studies of the expressed $Ca_V1.2$ channel for functional analysis. With this approach, we identified two in-vivo phosphorylation sites in the Hook domain of $Ca_V\beta$ subunits. Phosphomimetic and phosphoinhibitory mutations in the analogous sites differentially modulate the function of full-length $Ca_V1.2$ channels expressed in nonmuscle cells.

2. Experimental Procedures

2.1. Protein purification, and sample preparation

All animal procedures were conducted in compliance with the recommendations of the Institutional Animal Care and Use Committee of the University of Washington. Rabbit skeletal muscle $Ca_V1.1$ channels were purified as previously described [30]. Male New Zealand White rabbits (2.5 kg, Western Oregon Rabbit Co) were euthanized by lethal injection of pentobarbital, skeletal muscle was rapidly harvested, rinsed briefly in phosphate buffered saline (PBS, pH 7.4), snap frozen in liquid nitrogen, and stored at −80°C. All purification steps were carried out at 4°C in the presence of the following protease and phosphatase inhibitors: 1 μM aprotinin, 1 μM pepstatin, 10 μM leupeptin, 100 μM benzamidine, 1 mM phenanthroline, 10 μM E-64, 20 μg/μL soybean trypsin inhibitor, 0.5 mM $NaVO_4$, 100 nM microcystin, 10 nM cyclosporin A. $Ca_V1.1$ was purified using wheat germ agglutinin linked agarose (Vector Labs) and anion exchange DEAE Sephadex A-25 (GE Healthcare), chromatography [30, 31]. Pure protein was snap frozen in liquid nitrogen and stored at −80°C in single-use aliquots. For mass spectrometric analysis, 1-2.5 μg of pure protein was separated by SDS-PAGE, the band of interest was excised and subjected to in-gel trypsin (Gold, Promega) digestion by standard procedures (http://donatello.ucsf.edu/ingel.html); 1-3 pmol of tryptic peptides were analyzed by mass spectrometry.

2.2. In vitro phosphorylation

Pure $Ca_V1.1$ was first dephosphorylated with 5 U Calf Intestinal-alkaline Phosphatase (CIP, NEB) for 2 h at 30°C in assay buffer (20 mM Tris pH7.5, 10 mM $MgCl_2$, 2 mM DTT, 10 mM NaCl, 200 mM ATP) and phosphatase was quenched with 10 mM $NaVO_4$. Then $Ca_V1.1$ was phosphorylated with 100 U PKA (Sigma, from Bovine heart), 100 U CaMKII (NEB), or 25 U CK2 (NEB) for 2.5 h at 30°C in assay buffer (20 mM Tris pH 7.5, 10 mM

$MgCl_2$, 2 mM DTT, 10 mM NaCl, 200 mM ATP). Reactions were quenched, proteins were resolved by SDS-PAGE, subjected to in-gel digestion, and phosphate incorporation was assessed by LC-MS and LC-MS/MS.

2.3 Mass spectrometry

Mass spectrometry was performed using an Agilent 1100 series HPLC (Agilent Technologies) coupled to an LCQ Classic ion trap mass spectrometer (ThermoElectron). Peptides were loaded on to a Paradigm Platinum Peptide Nanotrap (Microm) then separated on a reverse-phase capillary column (10 cm × 75 μm, Jupiter Proteo C12, Phenomenex) with a linear gradient from 2%-40% acetonitrile in 40 min. One full mass scan was acquired (300-2000 Da) and then the four most intense peaks were selected for MS/MS analysis. The dynamic exclusion limit was set to exclude a given m/z after it had been sequenced 2x during a 90 sec interval. Mass spectra were analyzed using TurboSequest configured with the following parameters: a peptide mass tolerance of 2.5 Da (avg), a fragment ion mass tolerance of 1.0 Da (avg), differential modification on S/T/Y +80 Da, and allowance of two incomplete cleavages. All MS/MS peak assignments were manually validated. The relative abundance of the modified forms for each peptide was determined using the ICIS peak detection method (Xcalibur) for the indicated extract ions. The percentages were calculated based on the sum of integrated peak areas for all detected modified forms of the peptide.

2.4. cDNA constructs

To construct mutants $Ca_V\beta_{2b}^{S152A/E}$ and $Ca_V\beta_{2b}^{T164A/D}$ mutagenic primers were designed that contained an internal HindIII restriction site. $Ca_V\beta_{2b}^{S152A/E}$ and $Ca_V\beta_{2b}^{T164A/D}$ were all amplified in a two-phase manner, using a SacII-XhoI cDNA fragment of $Ca_V\beta_{2b}$ or $Ca_V1.2$ in pBluescript SK+. Phase I generated the 5′ and the 3′ arms using the WT DNA template. PCR products were gel purified. Phase II combined the 5′ and 3′ arms to serve as both initial primers and template. PCR products were precipitated, washed, dried, and resuspended. PCR products and vector were cut with Sac II and Xho I and isolated by ethanol precipitation. The digested vector was treated with calf alkaline phosphatase (CIP, NEB). Digested DNA was run out on a 1.25% agarose gel. Fragment bands were excised and purified either by Spin-X column (Fisher Scientific) or QIAQuick (QIAGEN). Fragments were ligated (Fast-Link, Epicentre). A negative control of vector and no insert was run at the same time. Ligation mixtures were then transformed into competent DH5 cells and samples were plated onto LB plates overnight. DNA was extracted from mutant colonies by basic SDS/sodium acetate method. Samples were screened by cutting with restriction enzymes whose recognition sites were silently built into the mutation primer. Positive samples were further purified (Quantum miniprep kit, Bio-Rad Laboratories) and sequenced (BigDye, ABI). When the sequences were confirmed to be correct, DNA from the original mini-prep was retransformed, amplified, and extracted (QUANTUM maxiprep kit, Bio-Rad Laboratories). Each mutant DNA in pBluescript SK+ (Stratagene) and the full-length WT $Ca_V\alpha1.2$ subunit in pCDNA3 (Stratagene) were digested with Sac II and Xho I, ligated, and subcloned. Samples were sequenced again to confirm the sequence of the final construct.

2.5. Cell culture

TsA-201 cells were grown to 80% confluence and transfected with an equimolar ratio of cDNA encoding $Ca_V1.2$ full-length (FL), $Ca_V\beta_{2b}$ or mutated $Ca_V\beta_{2b}$ ($Ca_V\beta_{2b}^{S152A/E}$ and $Ca_V\beta_{2b}^{T164A/D}$, $Ca_V\alpha_2\delta_1$, and CD8 as a cell surface marker (EBO-pCD-Leu2; American Type Culture Collection) using Fugene (Roche). 15–24 h after transfection, cells were suspended, plated at low density in 35-mm dishes, and incubated at 37°C in 10% CO_2 for at least 17 h before recording using the whole-cell configuration of the patch clamp technique. Transiently transected cells were visualized with latex beads conjugated to an anti-CD8 antibody (Invitrogen).

2.6. Electrophysiology

Patch pipettes (2.5–3.5 MΩ) were pulled from micropipette glass (VWR Scientific) and fire-polished. Currents were recorded with an Axopatch 200B amplifier (MDS Analytical Technologies) and sampled at 5 kHz after anti-alias filtering at 2 kHz. Data acquisition and command potentials were controlled by Pulse (Pulse 8.50; HEKA), and data were stored for off-line analysis. Voltage protocols were delivered at 10s intervals unless otherwise noted, and leak and capacitive transients were subtracted using a P/4 protocol. Approximately 80% of series resistance was compensated with the voltage clamp circuitry.

For whole-cell voltage clamp recordings of $Ca_V1.2$ current in tsA-201 cells with Ba^{2+} or Ca^{2+} as a charge carrier ($I_{CaV1.2}$(Ba/Ca)), the extracellular bath solution contained (in mM): 10 $BaCl_2$ (or 1.8 mM $CaCl_2$), 140 Tris, 2 $MgCl_2$, and 10 D-glucose, titrated to pH 7.3 with $MeSO_4$. The intracellular solution contained (in mM): 130 CsCl, 10 HEPES, 4 MgATP, 1 $MgCl_2$, and 10 EGTA titrated to pH 7.3 with CsOH [32]. When Na^+ was used as charge carrier ($I_{CaV1.2}$(Na)), the extracellular solution contained (in mM): 150 NaCl, 10 HEPES, 0.2 $MgCl_2$, 0.25 μM EDTA, and 10 D-glucose titrated to pH 7.3 with $MeSO_4$. The intracellular solution contained (in mM): 150 CsOH, 110 glutamate, 20 HCl, 10 HEPES, 5 TrisATP, 4.3 $MgCl_2$, and 10 EGTA titrated to pH 7.6 with CsOH [32].

2.7. Data analysis

Voltage-clamp data were compiled and analyzed using Igor (IGOR Pro version 5.0, Wavemetrics Inc.) and Excel (Excel 97, Microsoft). For measurement of $Ca_V1.2$ *I-V* relationship and voltage dependence of activation, peak step currents were measured from a 20 ms depolarization to potentials between −50 and 80 mV, while tail currents were measured during the subsequent repolarization to −40 mV. For the measurement of the voltage dependence of inactivation, 4-s depolarizations to potentials from −80 to 30 mV were applied to inactivate a fraction of $Ca_v1.2$ channels. A standard test pulse of 30 ms to 30 mV was applied, and peak tail currents were measured during repolarization to −40 mV immediately following the test pulse. Activation and inactivation data were fit to a Boltzmann function (Prism 5.0d, GraphPad Software Inc.). To normalize for variation in transfection efficiency currents were normalized to the gating charge (Q_{on})[33]. For $Ca_V1.2$ inactivation, currents were elicited by test pulses between −80 mV to 30 mV of 1000 ms duration. To quantify inactivation, peak currents elicited by 1000 ms depolarizations to 0 mV were normalized to 1.0, and the fraction of peak current remaining at the end of the voltage pulse (r_{1000}) was measured. Pulses were applied every 30 s.

All data are presented as mean ± SEM. The statistical significance of differences between the various experimental groups was evaluated using the Student's *t* test or one-way ANOVA, followed by the Newman-Keuls post-test; p-values are presented in the text.

Results

3.1. Sites of phosphorylation of $Ca_V\beta_{1a}$ subunits

$Ca_V1.1$ channels in partially purified preparations of skeletal muscle transverse tubule membranes were labeled with [^{3}H]isradipine, solubilized with digitonin, and purified by chromatography on wheat germ agglutinin-Sepharose and DEAE-Sepharose [30, 31, 34]. The purified protein was concentrated by re-chromatography on wheat germ agglutinin-Sepharose, and the subunits were separated by SDS-PAGE (Fig. 1A). The band at approximately 55 kDa containing the $Ca_V\beta_{1a}$ subunit was excised, extracted, and prepared for mass spectrometry as described under Experimental Procedures (Fig. 1A). Analysis of the mass spectra revealed phosphorylation of Ser^{193} in the peptide Ser^{186}-Arg^{202}, which has a molecular mass of 820.4 without phosphorylation and 860.4 after phosphorylation (Fig. 2). In addition, we observed phosphorylation of Thr^{205} in the peptide Arg^{203}-Lys^{240} (Fig. 3). Both of these sites are located in the HOOK domain, which connects the SH3 domain and the guanylate kinase domain (Fig. 1B). The functional role of the HOOK domain is unknown.

Ser^{193} is in the amino acid sequence -SSLGD/E-, which is conserved in all four $Ca_V\beta$ subunits (Fig. 1B). The analogous sequence in $Ca_V\beta_{2b}$, the most abundant isoform in mammalian heart [35], contains the potential phosphorylation target Ser^{152}. The consensus sequence SXXD/E is a potential site for phosphorylation by casein kinase II (www.phosphosite.org). However, the level of phosphorylation of this site in vivo was low, and casein kinase II treatment did not increase phosphorylation of this peptide in purified $Ca_V1.1$ channels in vitro (Fig. 4). This site may be phosphorylated at a low level by another kinase in vivo, or it may only be phosphorylated by casein kinase II under specific physiological conditions in vivo.

Thr^{205} is in the amino acid sequence -RRTP-, which is a consensus for phosphorylation by PKA (Fig. 5). The Hook domain of $Ca_V\beta_1$ was previously shown to be phosphorylated by PKA at Thr^{205} in vitro in purified preparations of skeletal muscle calcium channels [18], and bioinformatic analysis suggests that $Ca_V\beta_1{}^{T205}$ is within a strong consensus sequence for PKA/CaMKII/PKC phosphorylation [18, 27]. This site is conserved in $Ca_V\beta1$, $Ca_V\beta2$, and $Ca_V\beta4$, although the consensus is less optimal for phosphorylation in $Ca_V\beta4$ because one of the two Arg residues is replaced by Phe (Fig. 1B). Incubation of purified $Ca_V1.1$ channels with PKA in vitro substantially increased the phosphorylation of Thr^{205} (Fig. 5), consistent with a significant physiological role of phosphorylation of this site. This sequence is conserved as -RKST- in $Ca_V\beta_{2b}$ with Thr^{164} as the phosphorylated residue.

3.2. Modulation of $Ca_V1.2$ channel activity by mutation of Ser^{152} in $Ca_V\beta_{2b}$

$Ca_V1.2$ channels have multiple sites of phosphorylation on their pore-forming α_1 subunits, which complicates interpretation of experiments that manipulate phosphorylation of $Ca_V\beta$

subunits by activation of protein kinases. Moreover, the kinase(s) that phosphorylate Ser^{193}/Ser^{152} in vivo are unknown. Therefore, to probe potential functional effects for phosphorylation of this site in $Ca_V1.2$ channel regulation, we created phosphomimetic and phosphoinhibitory mutants by substitution of Glu and Ala, respectively, for Ser^{152}. We expressed $Ca_V1.2$ channels with the $Ca_V\beta_{2b}$ mutants $Ca_V\beta_{2b}^{S152A}$ and $Ca_V\beta_{2b}^{S152E}$ in human embryonic kidney tsA-201 cells and processed them for electrophysiological analysis. The phosphoinhibitory mutation, $Ca_V\beta_{2b}^{S152A}$, increased $Ca_V1.2$ channel current amplitude, whereas phosphomimetic mutation, $Ca_V\beta_{2b}^{S152E}$, decreased $Ca_V1.2$ current amplitude relative to $Ca_V\beta_{2b}^{WT}$ (Fig. 7A). The $Ca_V1.2$ current amplitudes were −6.49 ± 0.9 pA/fC (n = 8) and −2.95 ± 0.88 pA/fC (n = 6) ($P < 0.05$), for $Ca_V\beta_{2b}^{S152A}$ and $Ca_V\beta_{2b}^{S152E}$, respectively. The phosphomimetic mutation $Ca_V\beta_{2b}^{S152E}$ also shifted the *I/V* relationship and the voltage dependence of activation and inactivation to more positive membrane potentials, whereas the phosphoinhibitory mutation $Ca_V\beta_{2b}^{S152A}$ had the opposite effects (Fig. 6A-C). The activation $V_{1/2}$ values were −11.1 ± 2.2 mV (n = 8) and 7.5 ± 5.2 mV (n = 6) ($P < 0.05$), for $Ca_V\beta_{2b}^{S152A}$ and $Ca_V\beta_{2b}^{S152E}$, respectively, whereas the activation $V_{1/2}$ for $Ca_V\beta_{2b}^{WT}$ was intermediate at −1.0 ± 2.7 mV (n = 12). Similar results were observed with these phosphomimetic mutations inserted into $Ca_V\beta_{1b}$. Overall, these results suggest that introduction of negative charge at this novel phosphorylation site in the HOOK domain of $Ca_V\beta$ subunits acts as a gating modifier to reduce opening probability of $Ca_V1.2$ channels and to impede the voltage-induced activation and inactivation gating of $Ca_V1.2$ channels.

3.3. Modulation of $Ca_V1.2$ channel activity by mutation of $Ca_V\beta_{2b}$ Thr^{164}

To probe the role of phosphorylation of Thr^{164} in $Ca_V1.2$ channel regulation, we expressed $Ca_V1.2$ channels with the phosphoinhibitory and phosphomimetic mutations $Ca_V\beta_{2b}^{T164A}$ and $Ca_V\beta_{2b}^{T164D}$ in tsA-201 cells and performed electrophysiological analysis in the presence of the physiological charge carrier Ca^{2+} (1.8 mM). These mutations did not have strong effects on the *I/V* relationship or the voltage dependence of activation and inactivation (Fig. 7). However, we observed enhanced rate and extent of inactivation of $Ca_V1.2$ channels with WT and $Ca_V\beta_{2b}^{T164D}$ subunits compared to $Ca_V\beta_{2b}^{T164A}$ subunits (Fig. 8A and B). Analysis of two-exponential fits of these results showed that these effects were primarily on the second time constant for inactivation (Table 1). The results for WT $Ca_V\beta$ were similar to T164D, suggesting that this site is at least partially phosphorylated when Ca^{2+} currents are measured in normal physiological medium. We also engineered this mutation in $Ca_V\beta_{2a}$ to test if this effect would be present with a $Ca_V\beta$ subunit that confers decreased inactivation to $Ca_V1.2$ channels because of its membrane tethering by N-terminal palmitoylation [36]. $Ca_V1.2$ channels with $Ca_V\beta_{2a}^{T164A}$ or $Ca_V\beta_{2a}^{T164D}$ mutants had similar inactivation properties (Fig. 8C and D; Table 1). These results suggest that negative charge at $Ca_V\beta_{2b}^{T164}$ enhances the transition of $Ca_V1.2$ channels from open to inactivated state by accelerating the second rate constant governing this inactivation transition and that N-terminal palmitoylation of the $Ca_V\beta_{2a}$ subunit [36] overrides this effect.

Both voltage-dependent inactivation and Ca^{2+}-dependent inactivation contribute substantially to the inactivation of $Ca_V1.2$ channels when Ca^{2+} is the charge carrier. In order to assess the effects of the $Ca_V\beta_{2b}^{T164}$ mutations on voltage-dependent inactivation of $Ca_V1.2$ channels specifically, we used Na^+ as charge carrier [32]. We did not observe any

significant difference in voltage-dependent inactivation between $Ca_V\beta_{2b}^{T164D}$ and $Ca_V\beta_{2b}^{T164A}$ (Fig. 8E and F). These results suggest that negative charge at the position of $Ca_V\beta_{2b}^{T164}$ enhances the Ca^{2+}-dependent transition of $Ca_V1.2$ channels to the inactivated state with little effect on voltage-dependent inactivation. The results for WT $Ca_V\beta_{2b}$ revealed slightly faster inactivation (Fig. 8E and F), as if the hydroxyl group of the native Ser at this position makes an interaction that slightly enhances the rate of voltage-dependent inactivation, and this interaction is prevented in both mutants.

4. Discussion

4.1. nctional effects of phosphorylation sites in the C-terminal of $Ca_V\beta$ subunits

Previous studies have identified multiple sites of phosphorylation in the C-terminal domain of $Ca_V\beta$ subunits by protein kinases in vitro [18, 27-29]. PKA phosphorylates three sites in the C-terminal domain of $Ca_V\beta_{2b}$ subunits, and phosphorylation of these sites was reported to regulate the function of $Ca_V1.2$ channels expressed in nonmuscle cells [27]. Phosphatidylinositol-3 kinase phosphorylates a site in the C-terminal domain of the $Ca_V\beta_2$ subunit and regulates trafficking of the calcium channel complex to the plasma membrane [28]. Protein kinase G also phosphorylates a site in the C-terminal domain of the $Ca_V\beta_{2b}$ subunit and inhibits the activity of $Ca_V1.2$ channels expressed in nonmuscle cells [10]. Although these studies suggest essential functional roles for the C-terminal domain of $Ca_V\beta_2$ subunits, deletion of the C-terminal domain including all three proposed sites of regulatory phosphorylation has no effect in mice [6]. The resulting C-terminal knockout mice are viable, fertile, and have no apparent physiological deficits [6]. Moreover, stimulation of the L-type calcium current in ventricular myocytes from these mice is normal [6]. Thus, these C-terminal phosphorylation sites on $Ca_V\beta_2$ subunits do not have essential functional roles that have been demonstrated in vivo. It is not known whether other $Ca_V\beta$ subunits can effectively compensate for loss of regulation by phosphorylation at these sites in the $Ca_V\beta_2$ subunit, but $Ca_V\beta$ subunits do compensate for each other when the complete genes are deleted [37]. Further work is required to determine whether the functional effects of phosphorylation of the C-terminal domain of $Ca_V\beta_2$ subunits observed in vitro in transfected nonmuscle cells are also important in vivo.

4.2. Phosphorylation sites in the Hook domain of $Ca_V\beta_{2b}$ subunits

Unexpectedly, our mass spectrometry analysis did not detect phosphorylation of the C-terminal domain of the $Ca_V\beta_{1a}$ subunit, but we found two previously unidentified sites of in-vivo phosphorylation in the Hook domain: Thr^{205} and Ser^{193}. These sites are located far from the site of interaction of $Ca_V\beta$ subunits α_1 subunits (Fig. 9, AID) and far from the previously identified sites of phosphorylation in the C-terminal region. Thr^{205} was identified as a PKA phosphorylation site by in vitro phosphorylation with [γ^{32}P]ATP in early biochemical studies of purified $Ca_V1.1$ channels [18], and we confirmed those results with mass spectrometry in this work. Ser^{193} was not previously identified as a site of protein phosphorylation of $Ca_V\beta_{1a}$ in biochemical studies, and the kinase that is responsible for its phosphorylation in vivo remains unknown.

Functional studies of $Ca_V1.1$ channels are made difficult by poor cell-surface expression in nonmuscle cells. Therefore, we analyzed the potential functional effects of phosphorylation of the homologous Ser^{152} and Thr^{164} residues through studies of mutants of the $Ca_V\beta_{2b}$ subunit co-expressed with $Ca_V1.2$ channels in human embryonic kidney tsA-201 cells. The functional effects of phosphomimetic and phosphoinhibitory mutations at these sites suggest complementary regulatory roles. Addition of a negative charge at Ser^{152} decreases peak $Ca_V1.2$ channel currents and shifts both activation and inactivation to more positive membrane potentials. Together, these effects would significantly decrease channel activity. Because co-expression of $Ca_V\beta_{2b}$ subunits causes a negative shift in the voltage dependence of channel activation [38], addition of negative charge at this position by protein phosphorylation would oppose this functional effect of the $Ca_V\beta_{2b}$ subunit. In contrast, addition of negative charge at the position of Thr^{164} in $Ca_V\beta_{2b}$ subunits has no effect on the voltage dependence of activation or inactivation, but it significantly increases the rate of calcium-dependent inactivation. These results suggest possible interactions between the Hook domain in the $Ca_V\beta_{2b}$ subunit and the proximal C-terminal domain of the $Ca_V\alpha_1$ subunit where calcium-dependent inactivation is mediated by interaction of calcium/calmodulin with an IQ motif [15].

4.3. Possible physiological significance of phosphorylation of the Hook domain

Our results revealing functional effects of phosphomimetic mutations in the Hook domain are in agreement with previous work showing that the Hook domain of $Ca_V\beta$ can regulate Ca_V channel inactivation [39]. Deletion of the Hook domain of $Ca_V\beta_{2a}$ enhanced $Ca_V2.2$ channel inactivation suggesting that the Hook domain normally interacts with $Ca_V2.2$ α-subunit to impede $Ca_V2.2$ channel inactivation [39]. The $Ca_V\beta$ Hook domain was also shown to regulate the binding affinity of Gβγ to $Ca_V\beta$ subunits to regulate $Ca_V2.2$ channel activity [40]. It is possible that phosphorylation sites in the Hook domain could regulate the binding affinity of Gβγ for $Ca_V\beta$ subunits and thereby modulate their effects on $Ca_V2.2$ channel activity because the interaction sites for Gβγ and $Ca_V\beta$-subunits are located close to each other in the intracellular linker connecting domains I and II of $Ca_V\alpha_1$ subunits [41-45].

Determining the significance of phosphorylation of the Hook domain of $Ca_V\beta$-subunits for regulation of basal and PKA-stimulated activity of $Ca_V1.2$ channels is an important aim for future experiments, but will require a detailed analysis of the complex signaling network that controls the activity of this channel. The basal activity of $Ca_V1.2$ channels expressed as an autoinhibitory signaling complex with bound AKAP and PKA in nonmuscle cells is much reduced by mutations that prevent phosphorylation of Ser^{1700} and Thr^{1704}, which are located at the interface between the distal and proximal C-terminal domains of the $Ca_V\alpha_1$ subunit [23, 24]. Ser^{1700} is a substrate for phosphorylation by PKA and CaMKII, whereas Thr^{1704} is a substrate for casein kinase II [23, 24]. If phosphorylation of Ser^{152} in $Ca_V\beta_{2b}$ inhibits $Ca_V1.2$ channel activity, as implied by our results, this effect would oppose up-regulation of basal channel activity by phosphorylation at Ser^{1700} and Thr^{1704} in the $Ca_V\alpha_1$ subunit.

β-adrenergic stimulation of the heart in the fight-or-flight response leads to both increased contractility, which is caused by increased peak L-type calcium currents in atrial and

ventricular myocytes, and to increased beating rate, which is caused jointly by activation of hyperpolarization- and cyclic nucleotide-gated channels and $Ca_V1.3$ channels in the sino-atrial node [46, 47]. PKA stimulation of $Ca_V1.2$ channels expressed as an autoinhibitory signaling complex in nonmuscle cells is blocked by mutations that prevent phosphorylation of Ser^{1700} in the $Ca_V\alpha_1$ subunit [23], and mutation of Ser^{1700} and Thr^{1704} in mice greatly reduces the response to β-adrenergic stimulation in ventricular myocytes [25, 26]. If phosphorylation of Thr^{164} in the $Ca_V\beta_{2b}$ subunit has no effect on peak current, as implied by our results, this site of phosphorylation would not contribute directly to the up-regulation of $Ca_V1.2$ channel activity by PKA. However, increased beating rate in response to β-adrenergic stimulation of the heart requires shortening of the ventricular action potential. Enhanced activation of K_V channels by PKA phosphorylation is a well-documented mechanism contributing to shortening of the ventricular action potential during β-adrenergic stimulation of the heart [48]. However, phosphorylation of Thr^{164} in the $Ca_V\beta_{2b}$ subunit would increase the rate of calcium-dependent inactivation, shorten the L-type calcium current, and thereby contribute to shortening the plateau of the ventricular action potential. Knock-in mutations in mice will be require to rigorously test these potential physiological effects of phosphorylation of the Hook domain of $Ca_V\beta_{2b}$ subunits.

Acknowledgements

Research reported in this publication was supported by the National Heart, Lung, and Blood Institute (NHLBI) of the National Institutes of Health under award number R01HL085372. The content is solely the responsibility of the authors and does not necessarily represent the official views of the National Institutes of Health.

References

[1]. Dai S, Hall DD, Hell JW. Supramolecular assemblies and localized regulation of voltage-gated ion channels. Physiol Rev. 2009; 89:411–52. [PubMed: 19342611]

[2]. Catterall WA. Structure and regulation of voltage-gated Ca^{2+} channels. Annu Rev Cell Dev Biol. 2000; 16:521–55. [PubMed: 11031246]

[3]. Reuter H. Calcium channel modulation by neurotransmitters, enzymes and drugs. Nature. 1983; 301:569–74. [PubMed: 6131381]

[4]. Tsien RW, Bean BP, Hess P, Lansman JB, Nilius B, Nowycky MC. Mechanisms of calcium channel modulation by β-adrenergic agents and dihydropyridine calcium agonists. J Mol Cell Cardiol. 1986; 18:691–710. [PubMed: 2427730]

[5]. Trautwein W, Cavalie A, Flockerzi V, Hofmann F, Pelzer D. Modulation of calcium channel function by phosphorylation in guinea pig ventricular cells and phospholipid bilayer membranes. Circ Res. 1987; 61:I17–23. [PubMed: 2443271]

[6]. Blaich A, Welling A, Fischer S, Wegener JW, Kostner K, Hofmann F, et al. Facilitation of murine cardiac L-type $Ca_V1.2$ channel is modulated by calmodulin kinase II-dependent phosphorylation of S1512 and S1570. Proc Natl Acad Sci U S A. 2010; 107:10285–9. [PubMed: 20479240]

[7]. Chen X, Piacentino V 3rd, Furukawa S, Goldman B, Margulies KB, Houser SR. L-type Ca^{2+} channel density and regulation are altered in failing human ventricular myocytes and recover after support with mechanical assist devices. Circ Res. 2002; 91:517–24. [PubMed: 12242270]

[8]. Chen X, Zhang X, Harris DM, Piacentino V 3rd, Berretta RM, Margulies KB, et al. Reduced effects of BAY K 8644 on L-type Ca^{2+} current in failing human cardiac myocytes are related to abnormal adrenergic regulation. Am J Physiol Heart Circ Physiol. 2008; 294:H2257–67. [PubMed: 18359894]

[9]. Schroder F, Handrock R, Beuckelmann DJ, Hirt S, Hullin R, Priebe L, et al. Increased availability and open probability of single L-type calcium channels from failing compared with nonfailing human ventricle. Circulation. 1998; 98:969–76. [PubMed: 9737516]

[10]. Yang L, Katchman A, Morrow JP, Doshi D, Marx SO. Cardiac L-type calcium channel ($Ca_V1.2$) associates with γ subunits. FASEB J. 2011; 25:928–36. [PubMed: 21127204]

[11]. Chu PJ, Robertson HM, Best PM. Calcium channel γ subunits provide insights into the evolution of this gene family. Gene. 2001; 280:37–48. [PubMed: 11738816]

[12]. Dick IE, Tadross MR, Liang H, Tay LH, Yang W, Yue DT. A modular switch for spatial Ca^{2+} selectivity in the calmodulin regulation of Ca_V channels. Nature. 2008; 451:830–4. [PubMed: 18235447]

[13]. De Jongh KS, Murphy BJ, Colvin AA, Hell JW, Takahashi M, Catterall WA. Specific phosphorylation of a site in the full-length form of the α 1 subunit of the cardiac L-type calcium channel by adenosine 3',5'-cyclic monophosphate-dependent protein kinase. Biochemistry. 1996; 35:10392–402. [PubMed: 8756695]

[14]. Peterson BZ, DeMaria CD, Adelman JP, Yue DT. Calmodulin is the Ca^{2+} sensor for Ca^{2+} -dependent inactivation of L-type calcium channels. Neuron. 1999; 22:549–58. [PubMed: 10197534]

[15]. Zuhlke RD, Pitt GS, Deisseroth K, Tsien RW, Reuter H. Calmodulin supports both inactivation and facilitation of L-type calcium channels. Nature. 1999; 399:159–62. [PubMed: 10335846]

[16]. Hulme JT, Lin TW, Westenbroek RE, Scheuer T, Catterall WA. β-adrenergic regulation requires direct anchoring of PKA to cardiac $Ca_V1.2$ channels via a leucine zipper interaction with A kinase-anchoring protein 15. Proc Natl Acad Sci U S A. 2003; 100:13093–8. [PubMed: 14569017]

[17]. Hulme JT, Konoki K, Lin TW, Gritsenko MA, Camp DG 2nd, Bigelow DJ, et al. Sites of proteolytic processing and noncovalent association of the distal C-terminal domain of $Ca_V1.1$ channels in skeletal muscle. Proc Natl Acad Sci U S A. 2005; 102:5274–9. [PubMed: 15793008]

[18]. De Jongh KS, Merrick DK, Catterall WA. Subunits of purified calcium channels: a 212-kDa form of α1 and partial amino acid sequence of a phosphorylation site of an independent β subunit. Proc Natl Acad Sci U S A. 1989; 86:8585–9. [PubMed: 2554320]

[19]. De Jongh KS, Warner C, Colvin AA, Catterall WA. Characterization of the two size forms of the α1 subunit of skeletal muscle L-type calcium channels. Proc Natl Acad Sci U S A. 1991; 88:10778–82. [PubMed: 1720551]

[20]. Hulme JT, Yarov-Yarovoy V, Lin TW, Scheuer T, Catterall WA. Autoinhibitory control of the $Ca_V1.2$ channel by its proteolytically processed distal C-terminal domain. J Physiol. 2006; 576:87–102. [PubMed: 16809371]

[21]. Hulme JT, Ahn M, Hauschka SD, Scheuer T, Catterall WA. A novel leucine zipper targets AKAP15 and cyclic AMP-dependent protein kinase to the C terminus of the skeletal muscle Ca^{2+} channel and modulates its function. J Biol Chem. 2002; 277:4079–87. [PubMed: 11733497]

[22]. Brunet S, Scheuer T, Catterall WA. Increased intracellular magnesium attenuates β-adrenergic stimulation of the cardiac $Ca_V1.2$ channel. J Gen Physiol. 2013; 141:85–94. [PubMed: 23250865]

[23]. Fuller MD, Emrick MA, Sadilek M, Scheuer T, Catterall WA. Molecular mechanism of calcium channel regulation in the fight-or-flight response. Sci Signal. 2010; 3:ra70. [PubMed: 20876873]

[24]. Emrick MA, Sadilek M, Konoki K, Catterall WA. β-adrenergic-regulated phosphorylation of the skeletal muscle $Ca_V1.1$ channel in the fight-or-flight response. Proc Natl Acad Sci U S A. 2010; 107:18712–7. [PubMed: 20937870]

[25]. Fu Y, Westenbroek RE, Scheuer T, Catterall WA. Basal and β-adrenergic regulation of the cardiac calcium channel $Ca_V1.2$ requires phosphorylation of serine 1700. Proc Natl Acad Sci U S A. 2014; 111:16598–603. [PubMed: 25368181]

[26]. Fu Y, Westenbroek RE, Scheuer T, Catterall WA. Phosphorylation sites required for regulation of cardiac calcium channels in the fight-or-flight response. Proc Natl Acad Sci U S A. 2013; 110:19621–6. [PubMed: 24218620]

[27]. Gerhardstein BL, Puri TS, Chien AJ, Hosey MM. Identification of the sites phosphorylated by cyclic AMP-dependent protein kinase on the β2 subunit of L-type voltage-dependent calcium channels. Biochem. 1999; 38:10361–70. [PubMed: 10441130]

[28]. Viard P, Butcher AJ, Halet G, Davies A, Nurnberg B, Heblich F, et al. PI3K promotes voltage-dependent calcium channel trafficking to the plasma membrane. Nat Neurosci. 2004; 7:939–46. [PubMed: 15311280]

[29]. Yang L, Liu G, Zakharov SI, Bellinger AM, Mongillo M, Marx SO. Protein kinase G phosphorylates $Ca_V1.2$ α_{1C} and β2 subunits. Circ Res. 2007; 101:465–74. [PubMed: 17626895]

[30]. Florio V, Striessnig J, Catterall WA. Purification and reconstitution of skeletal muscle calcium channels. Methods Enzymol. 1992; 207:529–46. [PubMed: 1382201]

[31]. Curtis BM, Catterall WA. Purification of the calcium antagonist receptor of the voltage-sensitive calcium channel from skeletal muscle transverse tubules. Biochem. 1984; 23:2113–8. [PubMed: 6329263]

[32]. Brunet S, Scheuer T, Catterall WA. Cooperative regulation of $Ca_V1.2$ channels by intracellular Mg2+, the proximal C-terminal EF-hand, and the distal C-terminal domain. J Gen Physiol. 2009; 134:81–94. [PubMed: 19596806]

[33]. Bean BP, Rios E. Nonlinear charge movement in mammalian cardiac ventricular cells. Components from Na and Ca channel gating. J Gen Physiol. 1989; 94:65–93. [PubMed: 2553859]

[34]. Takahashi M, Seagar MJ, Jones JF, Reber BF, Catterall WA. Subunit structure of dihydropyridine-sensitive calcium channels from skeletal muscle. Proc Natl Acad Sci U S A. 1987; 84:5478–82. [PubMed: 2440051]

[35]. Chu PJ, Larsen JK, Chen CC, Best PM. Distribution and relative expression levels of calcium channel β subunits within the chambers of the rat heart. J Mol Cell Cardiol. 2004; 36:423–34. [PubMed: 15010281]

[36]. Chien AJ, Carr KM, Shirokov RE, Rios E, Hosey MM. Identification of palmitoylation sites within the L-type calcium channel β2a subunit and effects on channel function. J Biol Chem. 1996; 271:26465–8. [PubMed: 8900112]

[37]. Burgess DL, Biddlecome GH, McDonough SI, Diaz ME, Zilinski CA, Bean BP, et al. β subunit reshuffling modifies N- and P/Q-type Ca^{2+} channel subunit compositions in lethargic mouse brain. Mol Cell Neurosci. 1999; 13:293–311. [PubMed: 10328888]

[38]. Perez-Reyes E, Castellano A, Kim HS, Bertrand P, Baggstrom E, Lacerda AE, et al. Cloning and expression of a cardiac/brain β subunit of the L-type calcium channel. J Biol Chem. 1992; 267:1792–7. [PubMed: 1370480]

[39]. Richards MW, Leroy J, Pratt WS, Dolphin AC. The HOOK-domain between the SH3 and the GK domains of $Ca_V\beta$ subunits contains key determinants controlling calcium channel inactivation. Channels (Austin). 2007; 1:92–101. [PubMed: 18690022]

[40]. Dresviannikov AV, Page KM, Leroy J, Pratt WS, Dolphin AC. Determinants of the voltage dependence of G protein modulation within calcium channel β subunits. Pflugers Arch. 2009; 457:743–56. [PubMed: 18651169]

[41]. Van Petegem F, Clark KA, Chatelain FC, Minor DL Jr. Structure of a complex between a voltage-gated calcium channel β-subunit and an α-subunit domain. Nature. 2004; 429:671–5. [PubMed: 15141227]

[42]. Herlitze S, Hockerman GH, Scheuer T, Catterall WA. Molecular determinants of inactivation and G protein modulation in the intracellular loop connecting domains I and II of the calcium channel α1A subunit. Proc Natl Acad Sci U S A. 1997; 94:1512–6. [PubMed: 9037084]

[43]. Zamponi GW, Bourinet E, Nelson D, Nargeot J, Snutch TP. Crosstalk between G proteins and protein kinase C mediated by the calcium channel α1 subunit. Nature. 1997; 385:442–6. [PubMed: 9009192]

[44]. Pragnell M, De Waard M, Mori Y, Tanabe T, Snutch TP, Campbell KP. Calcium channel β-subunit binds to a conserved motif in the I-II cytoplasmic linker of the α1-subunit. Nature. 1994; 368:67–70. [PubMed: 7509046]

[45]. Chen YH, Li MH, Zhang Y, He LL, Yamada Y, Fitzmaurice A, et al. Structural basis of the α1-β subunit interaction of voltage-gated Ca^{2+} channels. Nature. 2004; 429:675–80. [PubMed: 15170217]

[46]. Bers DM. Cardiac excitation-contraction coupling. Nature. 2002; 415:198–205. [PubMed: 11805843]

[47]. Mangoni ME, Couette B, Marger L, Bourinet E, Striessnig J, Nargeot J. Voltage-dependent calcium channels and cardiac pacemaker activity: from ionic currents to genes. Prog Biophys Mol Biol. 2006; 90:38–63. [PubMed: 15979127]

[48]. Terrenoire C, Clancy CE, Cormier JW, Sampson KJ, Kass RS. Autonomic control of cardiac action potentials: role of potassium channel kinetics in response to sympathetic stimulation. Circ Res. 2005; 96:e25–34. [PubMed: 15731462]

Highlights

- Ca^{2+} channel β subunits are phosphorylated on two sites in the Hook domain in vivo
- Ser^{152} in $Ca_V\beta_{2b}$ has a casein kinase II consensus sequence; Thr 164 is a PKA site
- Phosphomimetic mutation S152E in $Ca_V\beta_{2b}$ decreased peak current and shifted activation
- Phosphomimetic mutation T164D in $Ca_V\beta_{2b}$ increased Ca^{2+}-dependent inactivation
- Phosphorylation of sites in the Hook domain may regulate $Ca_V1.2$ channels in vivo

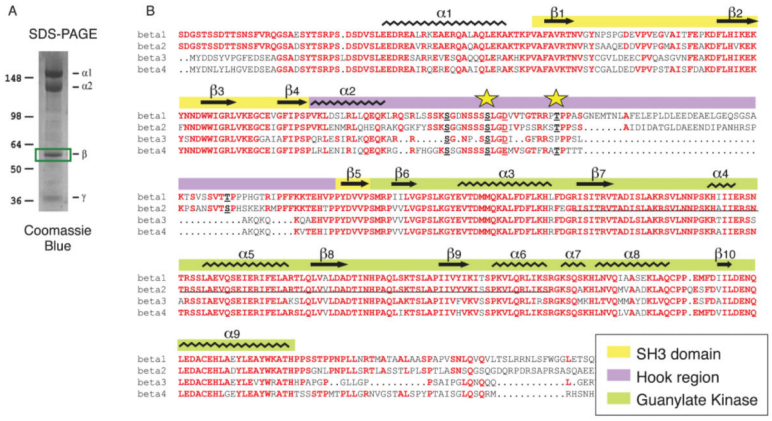

Figure 1. Sites of phosphorylation of $Ca_V\beta_{1a}$ in $Ca_V1.1$ channels in skeletal muscle

A. $Ca_V1.1$ channels were isolated from rabbit skeletal muscle as described in Experimental Procedures. Subunits were separated by SDS-PAGE and stained with Commassie blue. The protein band containing $Ca_V\beta_{1a}$ was excised as illustrated and used for analysis by mass spectrometry. **B.** Alignment of the amino acid sequences of the $Ca_V\beta$ subunits with secondary structure motifs indicated. Stars, Ser^{193} and Thr^{205}.

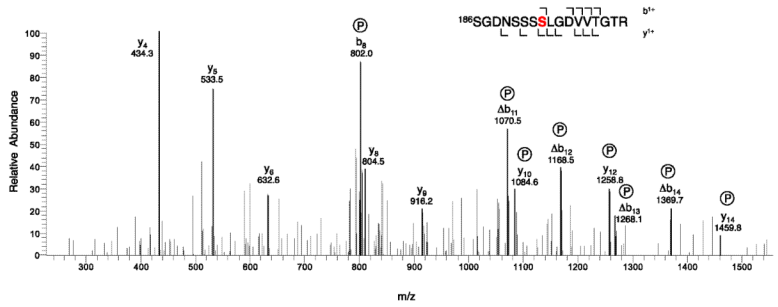

Figure 2. Identification of phosphorylated Ser^{193} by mass spectrometry

$Ca_V\beta_{1a}$ was isolated and analyzed as described in Experimental Procedures. The MS/MS spectrum of the phosphorylated tryptic peptides of $Ca_V\beta_{1a}$ (Parent MH^{2+} 860.4) is illustrated. For clarity, only the relevant portion of the spectrum is shown.

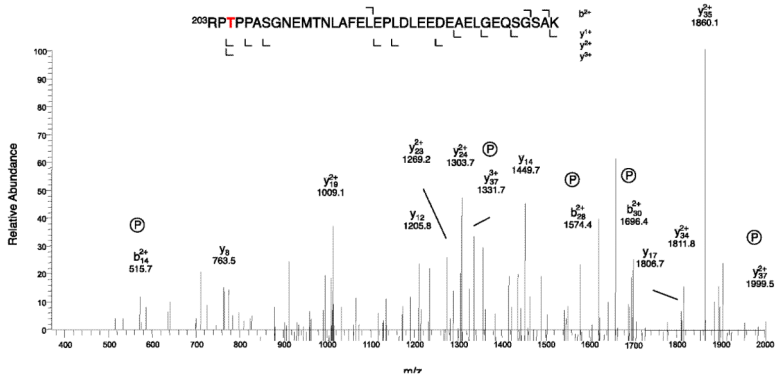

Figure 3. Identification of phosphorylated Thr^{205} by mass spectrometry

$Ca_V\beta_{1a}$ was isolated and analyzed as described in Experimental Procedures. The MS/MS spectrum of the phosphorylated tryptic peptides of $Ca_V\beta_{1a}$ (Parent MH^{3+} 1385.3) is illustrated. For clarity, only the relevant portion of the spectrum is shown.

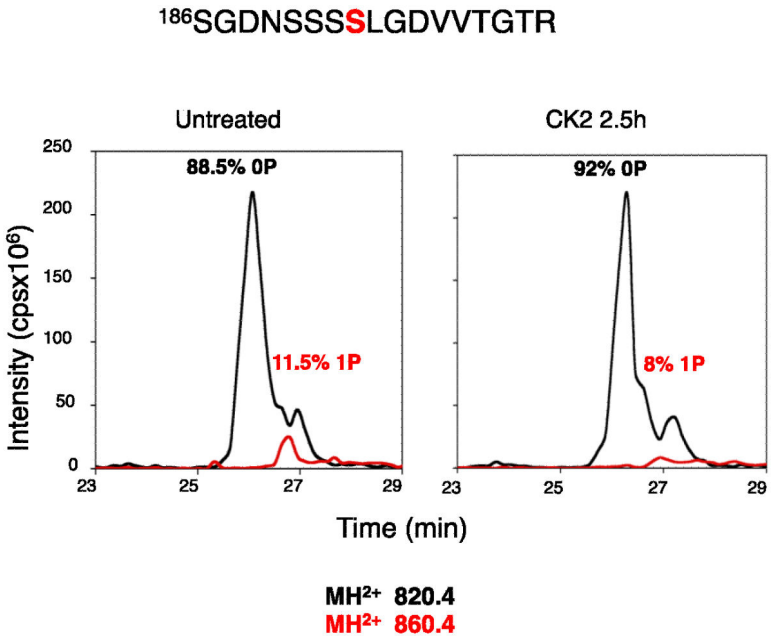

Figure 4. Phosphorylation of Ser^{193} by casein kinase II

Purified $Ca_V1.1$ channel was phosphorylated by purified casein kinase II as described in Experimental Procedures. The $Ca_V\beta_{1a}$ subunit was isolated by SDS-PAGE and analyzed by MS/MS. Integrated intensities of the peptide peaks representing unphosphoryated $Ca_V\beta_{1a}$ (0P) and phosphorylated $Ca_V\beta_{1a}$ (1P) are illustrated.

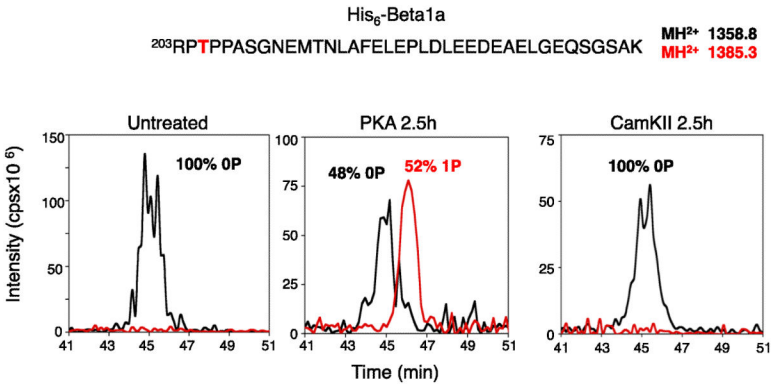

Figure 5. Phosphorylation of Thr^{205} by PKA

Purified $Ca_V1.1$ channel was phosphorylated by purified PKA as described in Experimental Procedures. The $Ca_V\beta_{1a}$ subunit was isolated by SDS-PAGE and analyzed by MS/MS. Integrated intensities of the peptide peaks representing unphosphoryated $Ca_V\beta_{1a}$ (0P) and phosphorylated $Ca_V\beta_{1a}$ (1P) are illustrated.

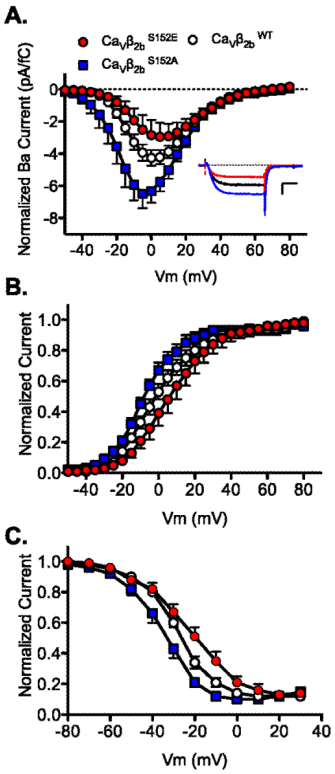

Figure 6. $Ca_V\beta_{2b}$ Hook-domain phosphorylation at Ser^{152} attenuates $Ca_V1.2$ current and shifts to the right the voltage dependence of activation of $Ca_V1.2$ channels

A. Effect of "phosphorylation mimetics" of a novel CK2 phosphorylation site in $Ca_V\beta_{2b}^{S152}$ on $Ca_V1.2$ channel *I-V* relationship. Ba^{2+} was the charge carrier and in order to normalize for $Ca_V1.2$ channel expression we divided the current amplitude by gating current (Q_{on})[32]. Inset, representative normalized typical current traces of $Ca_V\beta_{2b}^{S152A}$, $Ca_V\beta_{2b}^{S152E}$, and $Ca_V\beta_{2b}^{WT}$ taken at the peak of the *I-V* relationship (calibration bar: 5 ms and 2.5 pA/fC. The dotted line represents zero current level). **B.** $Ca_V\beta_{2b}^{S152A}$ shifts to the left the voltage dependence of activation of Ca 1.2 channels while $Ca_V\beta_{2b}^{S152E}$ shifts to the right the voltage dependence of activation of Ca 1.2 channels relative to $Ca_V\beta_{2b}^{WT}$. **C.** $Ca_V\beta_{2b}^{S152A}$ shifts to the left the voltage dependence of inactivation of $Ca_V1.2$ channels while $Ca_V\beta_{2b}^{S152E}$ shifted to the right the voltage dependence of inactivation of $Ca_V1.2$ channels relative to $Ca_V\beta_{2b}^{WT}$. Activation and inactivation parameters were: $Ca_V1.2$ FL^{WT}: $V_{1/2}$ = −1.0 ± 2.7 mV, k = −12.1 ± 1.0, n = 12 and $V_{1/2}$ = −28.0 ± 1.0 mV, k = 8.7 ± 0.6, n = 11; $Ca_V\beta_{2b}^{S152A}$: $V_{1/2}$ = − 11.1 ± 2.2 mV, k = −11.5 ± 2.2, n = 8 and $V_{1/2}$ = −35.0 ± 2.3 mV, k = 7.8 ± 0.5, n = 8; and $Ca_V\beta_{2b}^{S152E}$: $V_{1/2}$ = 7.5 ± 5.2 mV, k = − 11.7 ± 1.8, n = 6 and $V_{1/2}$ = −22.7 ± 3.0 mV, k = 12.3 ± 0.8, n = 6 for activation and inactivation parameters, respectively. There is a significant difference in $V_{1/2}$ of activation (≈18 mV, $P < 0.05$) and $V_{1/2}$ SS-inactivation (≈12 mV, $P < 0.01$) between $Ca_V\beta_{2b}^{S152A}$ and $Ca_V\beta_{2b}^{S152A}$.

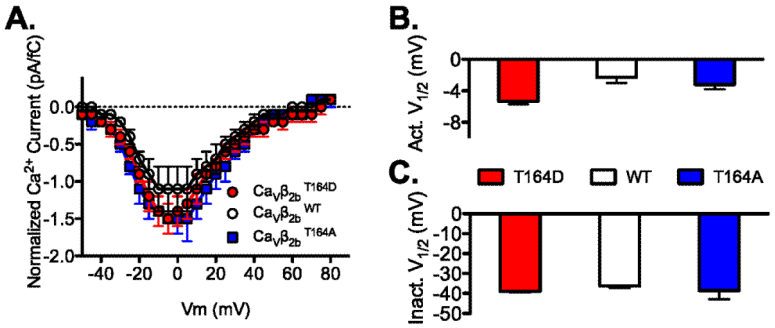

Figure 7. $Ca_V\beta_{2b}$ Hook-domain phosphorylation at Thr^{164} does not alter current amplitude, voltage dependence of activation or inactivation

A. Effect of "phosphorylation mimetics" of $Ca_V\beta_{2b}^{T164}$ on $Ca_V1.2$ *I-V* relationship. Ca^{2+} was the charge carrier and in order to normalize for $Ca_V1.2$ channel expression we divided the current amplitude by gating current (Q_{on})[32]. **B.** $Ca_V\beta_{2b}^{T164D}$ and $Ca_V\beta_{2b}^{T164A}$ did not alter the voltage dependence ofactivation of $Ca_V1.2$ channels, or **C.** voltage dependence of inactivation of $Ca_V1.2$ channels. $Ca_V\beta_{2b}^{WT}$ (n = 8, 8, 4), $Ca_V\beta_{2b}^{T164A}$ (n = 6, 6, 4) and $Ca_V\beta_{2b}^{T164D}$ (n = 9, 9, 6) for panel A, B and C, respectively. Activation (Act.) and inactivation (Inact.).

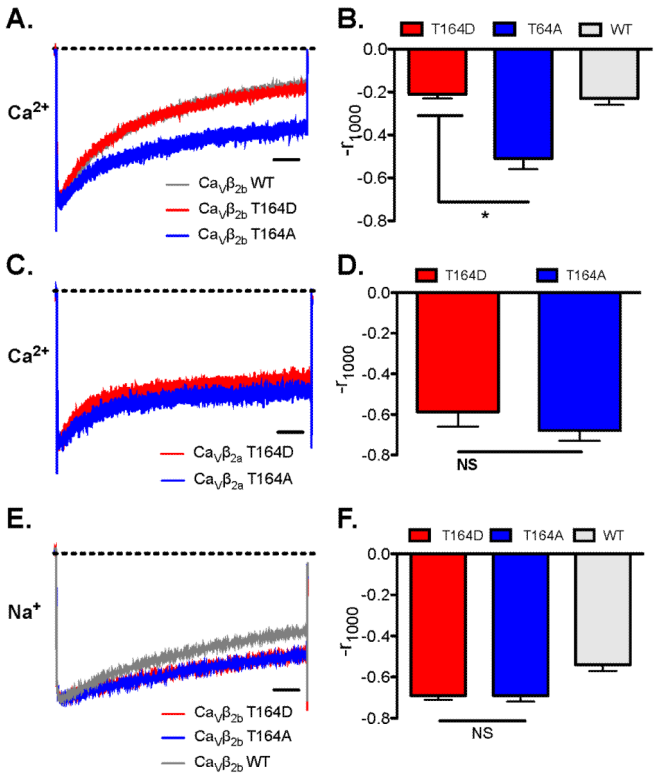

Figure 8. $Ca_V\beta_{2b}$ Hook-domain phosphorylation at Thr^{164} enhanced Ca^{2+}-dependent inactivation (CDI) of $Ca_V1.2$ channels

A. "Phosphorylation mimetics" $Ca_V\beta_{2b}{}^{T164D}$ enhances $Ca_V1.2$ channel inactivation. Currents were elicited by 1000 ms steps to 0 mV from a holding potential of −80 mV with Ca^{2+} as charge carrier. Average traces are represented. The dotted line in panels A, C, and E represent zero current level. $Ca_V\beta_{2b}{}^{T164D}$: n = 12 and $Ca_V\beta_{2b}{}^{T164A}$: n = 10. **B.** Bar graph of mean r_{1000} values measured with $Ca_V\beta_{2b}{}^{T164D}$ and $Ca_V\beta_{2b}{}^{T164A}$ were significantly different (* $P < 0.01$). **C.** Effects of $Ca_V\beta_{2a}$T164D and $Ca_V\beta_{2a}{}^{T164A}$ on $Ca_V1.2$ channel inactivation. $Ca_V\beta_{2a}{}^{T164D}$: n = 4; $Ca_V\beta_{2a}{}^{T164A}$: n = 4. **D.** Bar graph of mean r_{1000} values measured with $Ca_V\beta_{2a}{}^{T164D}$ and $Ca_V\beta_{2a}{}^{T164A}$ were not significantly different (NS). **E.** Effect of "phosphorylation mimetics" of $Ca_V\beta_{2a}{}^{T164}$ on $Ca_V1.2$ channel inactivation with Na^+ as charge carrier. $Ca_V\beta_{2b}{}^{T164D}$: n = 11; $Ca_V\beta_{2a}{}^{T164A}$: n = 8. **F.** Bar graph of mean r_{1000} values measured with $Ca_V\beta_{2a}{}^{T164A}$ with Na^+ as charge carrier were not significantly different.

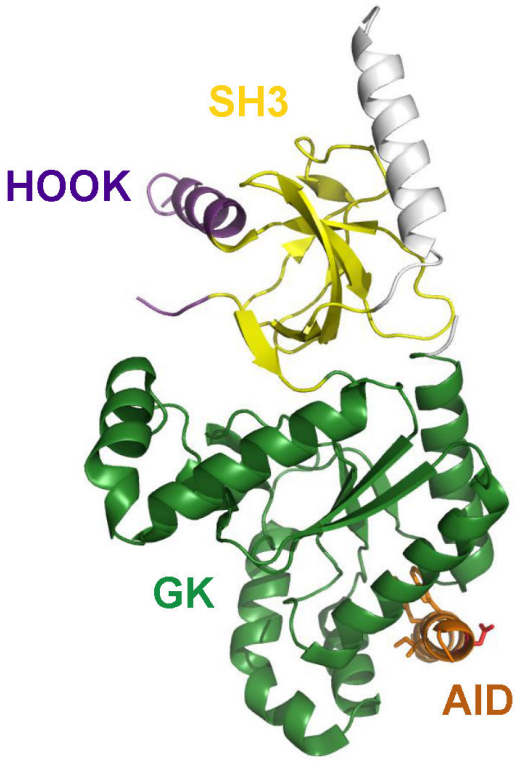

Figure 9. Structural model of the $Ca_V\beta$ subunit

The SH3 domain (yellow), HOOK domain (purple), Alpha Interaction Domain (AID, red), and Guanylate Kinase domain (GK, green) are illustrated in the indicated colors.

Table 1

	A1		t1 (msec)		A2		t2 (msec)		N
CaVb2b									
WT	0.53	±0.03	612	±54	0.45	±0.05	155	±37	13
T164A	0.34	±0.05	688	±77	0.29	±0.03	132	±24	10
T164D	0.56	±0.06	626	±155	0.37	±0.02	146	±34	12
CaVb2a									
T164A	0.27	±0.07	528	±331	0.27	±0.09	56	±15	4
T164D	0.21	±0.04	834	±89	0.33	±0.04	76	±5	4